Eddy heat fluxes from direct current measurements of the Antarctic Polar Front in Shag Rocks Passage

Graham J. Walkden,[1] Karen J. Heywood,[1] and David P. Stevens[2]

Received 22 November 2007; revised 15 January 2008; accepted 29 January 2008; published 18 March 2008.

[1] Determining meridional heat flux in the Southern Ocean is critical to the accurate understanding and model simulation of the global ocean. Mesoscale eddies provide a significant but poorly-defined contribution to this transport. An eighteen-month deep-water current meter array deployment in Shag Rocks Passage (53°S, 48°W) between May 2003 and November 2004 provides estimates of the eddy flux of heat across the Polar Front. We calculate a statistically nonzero (99% level), vertically coherent local poleward heat flux of 12.0 ± 5.8 kW m^{-2} within the eddy frequency band at ~2750 m depth. Exceeding previous deep-water estimates by up to an order of magnitude, this highlights the large spatial variation in flux estimates and illustrates that constriction of circumpolar fronts facilitates large eddy transfers of heat southwards. **Citation:** Walkden, G. J., K. J. Heywood, and D. P. Stevens (2008), Eddy heat fluxes from direct current measurements of the Antarctic Polar Front in Shag Rocks Passage, *Geophys. Res. Lett.*, *35*, L06602, doi:10.1029/2007GL032767.

1. Introduction

[2] The rate at which the ocean fluxes heat poleward is fundamental to our understanding of weather and climate systems and to our models thereof [*Charnock*, 1987]. The eddy contribution to this meridional transport is expected to be significant in the Southern Ocean, partly since the absence of continental boundaries rules out a flux in western boundary currents [*Gille*, 2003]. Since isopycnal surfaces tilt upward to the south and some outcrop within the Antarctic Circumpolar Current's (ACC) core, preferential along-isopycnal mixing can bring deep waters to the surface rather than permit cross-ACC heat transport. The Southern Ocean's high mesoscale variability can be partially attributed to the ACC's zonation [*Nowlin and Klink*, 1986]. Waves form and propagate along its fronts; meanders pinch off eddies, particularly from the Sub-Antarctic (SAF) and Polar Fronts (PF).

[3] The net ocean-to-atmosphere heat transfer south of the PF, Q, balances the sum of the heat fluxes due to mean geostrophic flow (excluding deep boundary currents) F_g, ageostrophic surface Ekman transport F_{Ek}, eddies F_e and deep boundary currents F_{bc} such that $Q = F_g + F_{Ek} + F_e + F_{bc}$ [*Nowlin and Klink*, 1986].

[4] From a hydrographic climatology, *de Szoeke and Levine* [1981] evaluated F_g at 0.00 ± 0.23 PW (PW = 10^{15} W) and inferred $F_{Ek} = 0.15 \pm 0.08$ PW, positive values directed equatorward. Therefore, $F_e + F_{bc}$ would need to supply −0.45 PW to balance the 0.30 ± 0.15 PW of heat lost south of the PF [*de Szoeke and Levine*, 1981]. *Heywood and Stevens* [2007] report a 0.033–0.061 PW southward heat transport within a modelled lower limb of the Southern Ocean's deep overturning circulation, which must include a contribution from F_{bc}. Existing long-term in situ studies of F_e have focused mainly on Drake Passage: *Bryden* [1979] estimating a cross-ACC poleward eddy heat transport of 6.7 kW m^{-2} (i.e. 6.7 kW per unit depth and pathlength of the ACC); *Sciremammano* [1980] estimating 9–28 kW m^{-2} after extension of the dataset; and *Nowlin et al.* [1985] estimating 3.7 kW m^{-2}. Away from geographical constriction, measurements south of Tasmania [*Phillips and Rintoul*, 2000] supplied a vertically-averaged 11.3 kW m^{-2} poleward eddy heat flux. Observations southeast of New Zealand [*Bryden and Heath*, 1985] yielded indeterminately-directed statistically insignificant poleward fluxes. Although these sparsely scattered estimates provide considerable local insight into the ACC's thermodynamics, it is unclear how representative they are of its entire pathlength. F_{bc} remains without direct estimation, but these F_e measurements alone are sufficient to meet the contribution required from $F_e + F_{bc}$.

2. Observations

[5] The ~2000 km-long North Scotia Ridge (NSR) lies between the Falkland Islands (Malvinas) and South Georgia. Its shallow 200–2000 m bathymetry blocks the circumpolar flow of deep waters [*Naveira Garabato et al.*, 2002]. The PF is constrained to cross the ridge through Shag Rocks Passage (SRP) [*Moore et al.*, 1999], a 180 km-wide, 3200 m-deep fracture zone between 49.6°W and 47.1°W. As part of the North Scotia Ridge Overflow Project (NSROP), a rotary current meter (RCM) array was deployed in SRP from May 2003 to November 2004. Six deep-water moorings, designated *Shag1a*, *Shag1b*, *Shag2a*, *Shag2b*, *Shag3a* and *Shag3b* spanned SRP from west to east across four mooring locations (Figure 1). The 'a' suffices identify moorings with RCMs elevated 30 and 100 m off the seabed whereas 'b' suffices label moorings with one RCM raised 400 m off the seafloor. Each of these nine Aanderaa RCM 8 yielded hourly-sampled current velocity, in situ temperature T and pressure. Table 1 summarises their positions, nominal depths and operational dates. Since the moorings extended no more than 400 m above the seabed, mooring

[1]School of Environmental Sciences, University of East Anglia, Norwich, UK.
[2]School of Mathematics, University of East Anglia, Norwich, UK.

0094-8276/08/2007GL032767$05.00

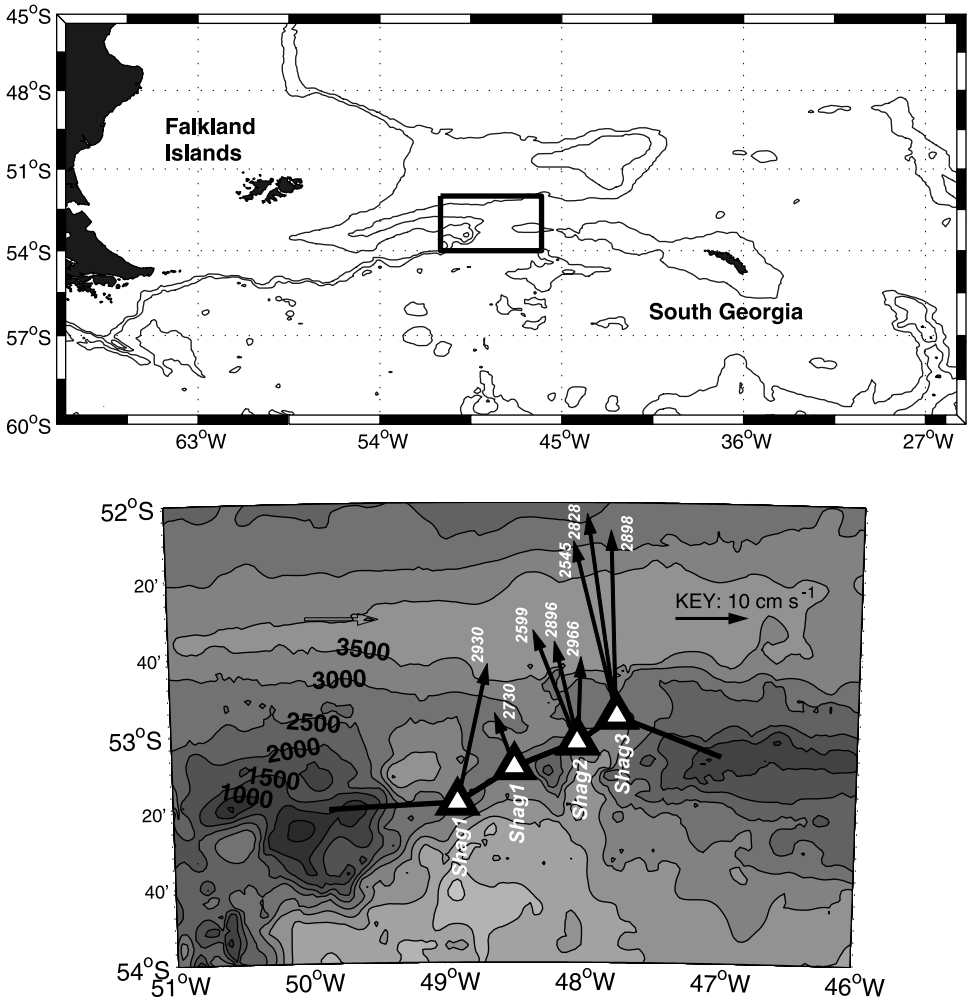

Figure 1. Regional map with 1000, 2000, 3000, and 4000 m depth contours (upper panel). The lower panel shows bottom topography at Shag Rocks Passage with a 500 m contour interval: Four mooring locations (triangles) with record-length mean velocities for the eight surviving RCMs (arrows) are annotated with instrument depth (m) in white. The mean flow clearly follows local bathymetric contours. Bathymetry from *Smith and Sandwell* [1997].

knock-down due to the strong currents was found to be negligible. Tides were removed from the velocity series using the T-TIDE harmonic analysis package [*Pawlowicz et al.*, 2002]. Analysis was restricted to the four most energetic tidal harmonics: O_1, K_1, M_2 and S_2. SRP's north-south orientation constrains tidal oscillations to be predominantly meridional. Tidal signatures comprised 0.7 ± 1.0 and 1.5 ± 1.2% of the total velocity variance in the meridional and zonal planes, respectively.

3. Heat Fluxes

[6] Careful definition of along-stream velocity $\hat{u}$ was required in order that cross-stream velocity $\hat{v}$, directed +90° relative to $\hat{u}$, could be determined. Following *Bryden*

Table 1. Positions, Nominal Depths, and Operational Dates of NSROP RCMs

Mooring	Latitude	Longitude	Depth, m	Height Above Bottom, m	Observational Dates	Record Length, d
Shag1a	53°18.251′S	48°54.828′W	2730	230	Instrument failed	0
Shag1a	53°18.251′S	48°54.828′W	2930	30	07/05/03 – 24/11/04	571
Shag1b	53°09.018′S	48°29.948′W	2366	400	07/05/03 – 02/09/04	514
Shag2a	53°02.510′S	48°02.313′W	2896	100	06/05/03 – 27/11/04	571
Shag2a	53°02.510′S	48°02.313′W	2966	30	06/05/03 – 26/11/04	570
Shag2b	53°02.510′S	48°02.770′W	2599	400	06/05/03 – 27/11/04	571
Shag3a	52°55.653′S	47°45.992′W	2828	100	05/05/03 – 15/11/04	559
Shag3a	52°55.653′S	47°45.992′W	2898	30	05/05/03 – 27/11/04	572
Shag3b	52°55.670′S	47°45.550′W	2545	400	05/05/03 – 27/11/04	572

Table 2. Temperature and Velocity Statistics in the 'Geographic' Coordinate Frame[a]

		Mean		Variance			
Mooring	Depth, m	$\bar{\hat{u}}$, cm s^{-1}	$\bar{T}$, deg C	$\overline{\hat{v}'^2}$, cm^2 s^{-2}	$\overline{\hat{u}'^2}$, cm^2 s^{-2} s^{-2}	$\overline{T'^2}$, deg C	$\overline{\hat{v}'T'}$, cm deg C s^{-1}
Shag1a	2930	14.5	1.1	24	131	0.06	−0.25
Shag1b	2366	5.9	1.6	83	114	0.04	−0.45
Shag2a	2896	10.6	1.0	122	160	0.04	−0.54
Shag2a	2966	8.7	0.8	146	116	0.04	−0.55
Shag2b	2599	12.3	1.0	93	125	0.04	−0.37
Shag3a	2828	20.9	0.7	62	121	0.02	−0.35
Shag3a	2898	19.0	0.6	57	82	0.05	−0.44
Shag3b	2545	18.4	0.9	49	122	0.04	−0.20

[a] $\hat{u}$ and $\hat{v}$ denote along-stream and cross-stream velocities, respectively. The $\bar{\hat{v}}$ is zero by definition.

[1979], velocity components were rotated into a 'geographic' co-ordinate frame relative to record-length mean flow directions (see Figure 1). We present temperature and velocity statistics in this reference frame in Table 2. Mean along-stream velocity $\bar{\hat{u}} \sim 14$ cm s$^{-1} > 0$, as required by the net circumpolar flow of the ACC, with variance $\overline{\hat{u}'^2} \sim 120$ cm^2 s^{-2}. Mean cross-stream velocities were zero by definition, with generally smaller variances $\overline{\hat{v}'^2} \sim 80$ cm^2 s^{-2}.

[7] The i^{th} instantaneous cross-stream heat flux is given by

$$\hat{Q}_i = \rho_0 C_p \hat{v}_i' T_i' \text{ W m}^{-2},$$

where $(.)'$ denotes a fluctuation value, $\rho_0 = 1041$ kg m^{-3} a representative water density and $C_p = 3904$ J kg^{-1} °C^{-1} the specific heat of seawater at constant pressure [*Nowlin et al.*, 1985]. The record-length mean eddy heat flux $\bar{\hat{Q}}$ must be negative if heat is to be transferred poleward (approximately eastward) in SRP.

[8] To isolate the mesoscale eddy contribution to the total observed cross-stream heat flux, we imposed an eddy frequency band of 40 hours < period < 90 days or 3/5 > frequency > 1/9 cpd on $\hat{v}$ and T records (Figure 2). The ninety-day cut-off neatly separated poleward fluxes at periods <90 days from an equatorward peak at ~120 days, which *Nowlin et al.* [1985] attribute to lateral shifts in frontal structure. Like *Phillips and Rintoul* [2000], we failed to observe the heat flux reduction seen for periods <6 days in data presented by *Nowlin et al.* [1985]. Record-length cross-PF $\hat{Q}$ means in the eddy frequency band are presented in Figure 3. All fluxes were statistically nonzero at the 99% level based on their $\hat{v} \times T$ zero-lag cross-correlation function [*Sciremammano*, 1979]. Five of six combinations of vertically separated pairs at the Shag2 and Shag3 sills showed significantly nonzero vertical magnitude-squared coherence in their eddy-band $\hat{Q}$ records. We took all eight estimates of the cross-stream heat flux and calculated their mean and standard deviation. Thus, our best record-length

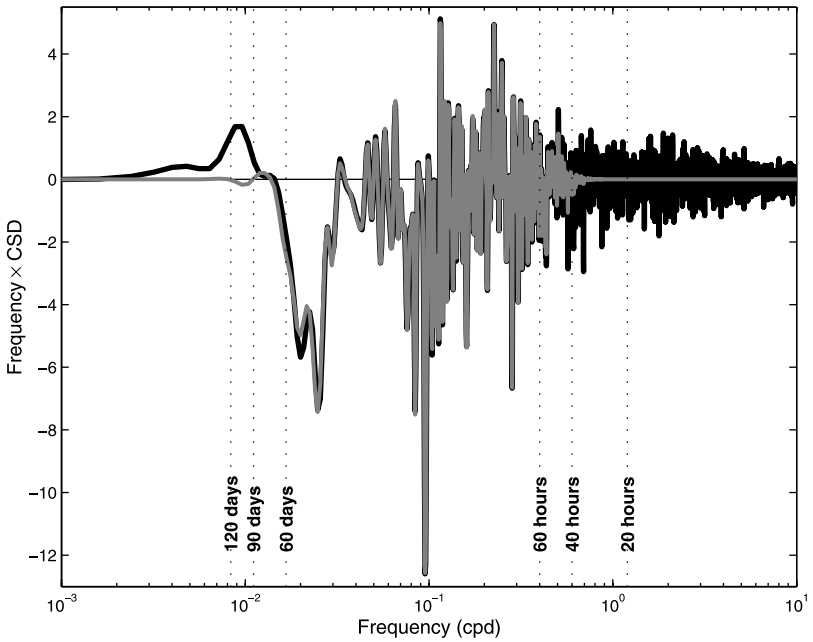

Figure 2. $\hat{v}' \times T'$ cospectral density estimates from 2366 m depth at Shag1b (black) and its 40 hours < period < 90 days bandpassed derivative (grey). The cospectral densities (CSDs) are multiplied by their corresponding frequencies such that areas under the abscissa are proportional to the heat flux. Positive [negative] regions represent equatorward [poleward] fluxes. Note the logarithmic frequency scale in cycles per day (cpd). Vertical dotted lines identify alternative passband limits used in a sensitivity test (see text).

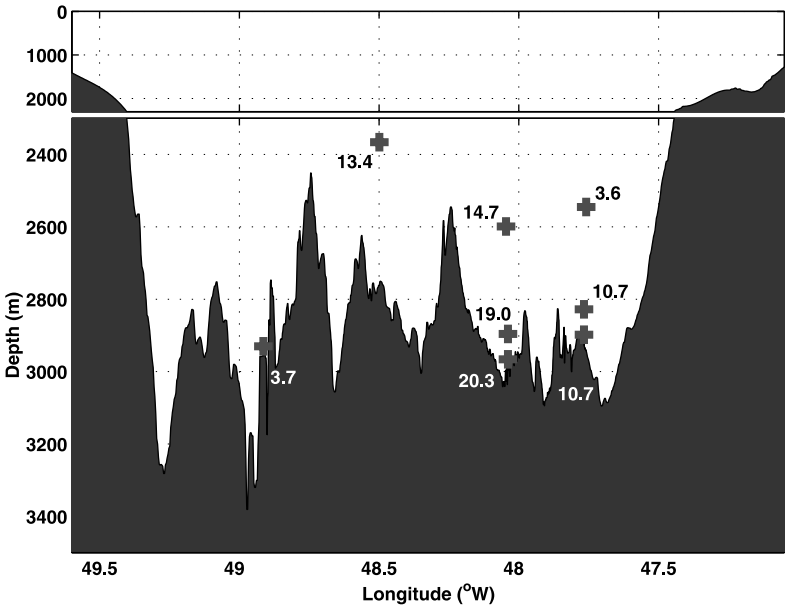

Figure 3. Record-length mean poleward eddy heat fluxes $\rho_0 C_p \overline{\hat{v}' T'}$ per unit depth and Polar Frontal length in kW m^{-2}, derived from 'geographic' co-ordinates and presented on the cross-section along the solid black line in Figure 1. Note the change of vertical scale between upper and lower panels.

mean eddy heat flux estimate was 12.0 ± 5.8 kW m^{-2} of a total (all-frequency) 14.0 ± 5.7 kW m^{-2} poleward transport.

[9] In defining their vectors, *Nowlin et al.* [1985] align $\hat{u}$ with the direction of the ninety-day low-passed current. Its success in central Drake Passage owes to the current flowing principally through-passage; the thermal wind, and therefore the baroclinic flow, parallelling this to within 5° [*Bryden and Pillsbury*, 1977]. Figure 1 demonstrates similarly constrained and invariant mean flow, suggesting this 'ninety-day' definition could work effectively in SRP. 'Ninety-day' co-ordinates provided statistically nonzero heat fluxes with four of the six eddy-band $\hat{Q}$ combinations demonstrating significant vertical coherence. By this method, 11.9 ± 6 kW m^{-2} of a total (all-frequency) 12.7 ± 6.7 kW m^{-2} heat transport lies within the eddy band.

[10] Increasing the passband width shown in Figure 2 to 20 hours < period < 120 days boosts record-length eddy fluxes averaged across the array by 8% in 'ninety-day' and 16% in 'geographic' co-ordinate frames. Conversely, reducing its span to 60 hours < period < 60 days decreases corresponding fluxes by 14 and 16%, respectively. The effect of altered passband definitions on eddy flux estimates is therefore eclipsed by their existing error bars.

[11] *Phillips and Rintoul* [2000] make successful flux estimates in the system defined by *Hall* [1986, 1989], whereby $\hat{u}$ represents the vertical current shear direction between 400 and 2000 dbar. This method was not replicable at the NSROP array because the depth range (2366–2966 m) it occupied was too small.

[12] Table 3 summarises previous local and zonally integrated cross-ACC eddy heat flux estimates. *Bryden*'s [1979] investigation in Drake Passage made no correction for mooring motion, so could include a ≤20% overestimation in pointwise transports. It was deemed statistically unreliable by *Sciremammano* [1980], citing the record length from which it was derived as too short and displaying too few heat flux events. The observations south of Tasmania were from another supposed choke point but *Phillips and Rintoul* [2000] deemed it to be an area of low (but growing) eddy energy. The highly constricted meridional temperature gradient in SRP partially explains its comparatively larger fluxes, since it makes eddies an especially effective heat transfer mechanism. Mesoscale turbulence is also heightened by the sensitivity of the ACC's potential vorticity to the shallow, rough bottom topography [*Gille*, 2003]. Thus the flow through SRP forms a strong component of interbasin exchange which, crucially, impacts on the global thermohaline circulation.

[13] The current meter studies in Table 3 demonstrate a profile of approximately exponentially decreasing eddy heat flux with depth. Assuming that it decreases with an e-folding scale H_e = 1000 m [*Gille*, 2003] (supported by flux profiles presented by *Phillips and Rintoul* [2000] and *Nowlin et al.* [1985]), that ocean depth H = 4 km and that the PF's circumpolar L = 28171 km [*Orsi et al.*, 1995], *Gille* [2003] gave the depth-integrated flux as

$$F_e = \oint \int_{z=-H}^{0} Q_e(z) dz dx \text{ W}$$
$$F_e = L H_e e^{-z_{ref}/H_e} Q_e(z_{ref}) \text{ W},$$

where $Q_e(z_{ref})$ denotes the eddy heat flux at the mean instrument depth z_{ref}, here −2750 m. The depth-integrated eddy heat flux in SRP is then −188 ± 91 MW m^{-1} (MW = 10^6 W) (i.e. per unit length of ACC). If representative of the entire circumpolar path, then the circumpolar value of F_e would be −5.3 ± 2.6 PW. If, alternatively, the flux profile were to remain constant with depth, these vertically- and circumpolarly-integrated fluxes would decrease to −48 ± 23 MW m^{-1} and −1.4 ± 0.7 PW, respectively. Even this lower limit would still more than balance the estimated 0.45 PW lost from the area south of the PF, closing the

Table 3. Statistically Significant Poleward Cross-ACC Eddy Heat Fluxes From Comparable Depths

Investigator	Location		Local Poleward Flux $-\bar{\hat{Q}}$, kW m^{-2}	Integrated Poleward Flux
		Current Meters		
Bryden [1979]	Drake Passage	2700 m	6.7	0.5
Sciremammano et al. [1980]	Drake Passage	1000–2500 m	17 (9–28)	—
Nowlin et al. [1985]	Drake Passage	2660 m	4.3	—
Johnson and Bryden [1989]	Drake Passage	580–3560 m	12	—
Phillips and Rintoul [2000]	143°E, 51°S	2240–3320 m	(2.1–3.1)	0.9
This Study	48°W, 53°S	2550–2990 m	12.0 (3.7–20.3)	5.3
		Hydrography		
de Szoeke and Levine [1981]	ACC	0–3000 m	—	0.45
		Altimetry		
Trenberth [1979]	ACC		—	1.0
Newton [1972]	ACC		—	0.29
Keffer and Holloway [1988]	ACC (53°S)		—	0.70
Stammer [1998]	ACC (53°S)		—	0.05
		Global Energy Balance		
Gordon and Owens [1987]	ACC		—	0.31

Southern Ocean heat budget. The exponentially-decaying integrated flux exceeds previous estimates (Table 3), both direct and indirect, by up to an order of magnitude. Modelled maximum heat transports have been observed in the southwest Indian Ocean ACC sector, where RCM coverage is poor [*Jayne and Marotzke*, 2002]. Indeed, *Gille* [2003] suggested that the major pathway for heat to enter the ACC may be through the area of high eddy energy downstream of the Agulhas Current retroflection, where Indian Ocean water meets the SAF and the strongest eddy heat fluxes are seen in float-derived measurements. This and the scattered, inhomogeneous nature of flux estimates suggest that pointwise transports from in situ measurements should not be extrapolated in this manner. Both *Sievers and Emery* [1978] and *Sciremammano* [1980] provide evidence for cold-core current rings shedding from the PF and migrating northward across the Polar Frontal zone, before being absorbed at the SAF. However, if eddies are advected downstream before being reassimilated by the PF, F_e would be overestimated by an integration of pointwise flux measurements. Thus, the fate of individual mesoscale disturbances should be determined before instantaneous fluxes are assigned to the net poleward transport F_e.

[14] *Johnson and Bryden* [1989] suggest that $\bar{\hat{Q}}$ should be proportional to the product of the mean average zonal wind stress $\overline{\tau^x} \sim 0.1$ N m^{-1} and the vertical potential temperature gradient $\partial T/\partial z = 4 \times 10^{-4}$ °C m^{-1} i.e.

$$\bar{\hat{Q}} = \rho_0 C_p \overline{\hat{v}' T'} = \frac{C_p \overline{\tau^x}}{f} \frac{\partial T}{\partial z} \text{ W m}^{-2},$$

where f represents the Coriolis parameter. By this relation, the minimum poleward heat flux required to balance the wind stress is 1.4 kW m^{-2}. Our observed eddy heat flux exceeds this by an order of magnitude. This suggests that momentum and heat transfer is spatially inhomogeneous and that SRP is a region of anomalously intense mesoscale activity.

4. Conclusions

[15] The heat fluxed poleward across the PF at ~2750 m in SRP was 14.0 ± 5.7 kW m^{-2}, of which 12.0 ± 5.8 kW m^{-2} was attributed to mesoscale eddies. This exceeded values at comparable depths in Drake Passage, south of Tasmania and southeast of New Zealand by up to an order of magnitude and more than matched the estimated 1.4 kW m^{-2} required to balance the zonal wind stress through interfacial form stress. This demonstrates how constriction of frontal structure can effect an especially large poleward eddy heat transfer. Assuming a 1000 m e-folding depth, −188 ± 91 MW m^{-1} would be fluxed through the whole watercolumn and 5.3 ± 2.6 PW southward across the entire PF by eddies. This more than balances the estimated 0.45 PW of heat lost to the atmosphere south of the PF but incorrectly assumes SRP to be representative of the PF's circumpolar path and that none of the eddies sampled were reassimilated downstream.

[16] The eddy flux of heat remains one of the most poorly quantified Southern Ocean parameters. This investigation contributes a locally accurate value to a zonally-undersampled series of synoptic measurements of the mesoscale field of the ACC. Given the poor coverage, it is crucial that, in future, fluxes be reliably determined from hydrographic or satellite sea-surface temperature data and assimilated into climate models.

[17] **Acknowledgments.** The NSROP was funded by the Natural Environment Research Council grant NER/G/S/2001/00006 through the Antarctic Funding Initiative. We thank Nicole Nicholls for her work calibrating and processing the raw dataset and Alberto Naveira Garabato for useful discussions. Alex Tate kindly provided multibeam bathymetry from the British Antarctic Survey Marine Geophysical Database.

References

Bryden, H. L. (1979), Poleward heat flux and conversion of available potential in Drake Passage, *J. Mar. Res.*, *37*, 1–22.

Bryden, H. L., and R. A. Heath (1985), Energetic eddies at the northern edge of the Antarctic Circumpolar Current, *Prog. Oceanogr.*, *14*, 65–87.

Bryden, H. L., and R. D. Pillsbury (1977), Variability of deep flow in the Drake Passage from year-long current measurements, *J. Phys. Oceanogr.*, *7*, 803–810.

Charnock, H. Q. (1987), Ocean currents and meridional transfers, *Q. J. R. Meteorol. Soc.*, *113*, 3–18.

de Szoeke, R. A., and M. D. Levine (1981), The advective flux of heat by geostrophic motions in the Southern Ocean, *Deep Sea Res., Part A*, *28*, 1057–1085.

Gille, S. T. (2003), Float observations of the Southern Ocean. part II: Eddy fluxes, *J. Phys. Oceanogr.*, *33*, 1182–1196.

Gordon, A. L., and W. B. Owens (1987), Polar oceans, *Rev. Geophys.*, *25*, 227–233.

Hall, M. M. (1986), Horizontal and vertical structure of the Gulf Stream velocity field at 68°W′, *J. Phys. Oceanogr.*, *16*, 1814–1828.
Hall, M. M. (1989), Velocity and transport structure of the Kuroshio Extension at 35°N, 152°E, *J. Geophys. Res.*, *94*, 14,445–14,459.
Heywood, K. J., and D. P. Stevens (2007), Meridional heat transport across the Antarctic Circumpolar Current by the Antarctic Bottom Water overturning cell, *Geophys. Res. Lett.*, *34*, L11610, doi:10.1029/2007GL030130.
Jayne, S. R., and J. Marotzke (2002), The oceanic eddy heat transport, *J. Phys. Oceanogr.*, *32*, 3328–3345.
Johnson, G. C., and H. L. Bryden (1989), On the size of the Antarctic Circumpolar Current, *Deep Sea Res., Part A*, *36*, 39–53.
Keffer, T., and G. Holloway (1988), Estimating Southern Ocean eddy flux of heat and from satellite altimetry, *Nature*, *332*, 624–626.
Moore, J. K., M. R. Abbott, and J. G. Richman (1999), Location and dynamics of the Antarctic Polar Front from satellite sea surface temperature data, *J. Geophys. Res.*, *104*, 3059–3073.
Naveira Garabato, A. C., K. J. Heywood, and D. P. Stevens (2002), Modification and pathways of Southern Ocean deep waters in the Scotia Sea, *Deep Sea Res., Part I*, *49*, 681–705.
Newton, C. W. (1972), Meteorology of the Southern Hemisphere, *Meteorol. Monogr.*, *13*, 215–246.
Nowlin, W. D., Jr., and J. M. Klink (1986), The physics of the Antarctic Circumpolar Current, *Rev. Geophys.*, *24*, 469–491.
Nowlin, W. D., Jr., S. J. Worley, and T. Whitworth III (1985), Methods for making point estimates of eddy heat flux as applied to the Antarctic Circumpolar Current, *J. Geophys. Res.*, *90*, 3305–3324.
Orsi, A. H., T. Whitworth III, and W. D. Nowlin Jr. (1995), On the meridional extent and fronts of the Antarctic Circumpolar Current, *Deep Sea Res., Part I*, *42*, 641–673.
Pawlowicz, R., B. Beardley, and S. Lentz (2002), Classical tidal harmonic analysis including error estimates in MATLAB using T_TIDE, *Comput. Geosci.*, *28*, 929–937.
Phillips, H. E., and S. R. Rintoul (2000), Eddy variability and energetics from direct current measurements in the Antarctic Circumpolar Current south of Australia, *J. Phys. Oceanogr.*, *30*, 3050–3076.
Sciremammano, F., Jr. (1979), A suggestion for the presentation of correlations and their significance levels, *J. Phys. Oceanogr.*, *9*, 1273–1276.
Sciremammano, F., Jr. (1980), The nature of the poleward heat flux due to low-frequency current fluctuations in Drake Passage, *J. Phys. Oceanogr.*, *30*, 3212–3222.
Sievers, H. A., and W. J. Emery (1978), Variability of the Antarctic Polar Frontal Zone in the Drake Passage—summer 1976–1977, *J. Geophys. Res.*, *83*, 3010–3022.
Smith, W. H. F., and D. T. Sandwell (1997), Global sea floor topography from satellite altimetry and ship depth soundings, *Science*, *277*, 1956–1962.
Stammer, D. (1998), On eddy characteristics, eddy transports, and mean flow properties, *J. Phys. Oceanogr.*, *28*, 727–739.
Trenberth, K. E. (1979), Mean annual poleward energy transports by the oceans in the Southern Hemisphere, *Dyn. Atmos. Oceans*, *4*, 57–64.

K. J. Heywood and G. J. Walkden, School of Environmental Sciences, University of East Anglia, Norwich NR4 7TJ, UK. (g.walkden@uea.ac.uk)
D. P. Stevens, School of Mathematics, University of East Anglia, Norwich NR4 7TJ, UK.